A Decentralized Model Reference Adaptive Controller for Large-Scale Systems

Prabhakar R. Pagilla, *Member, IEEE*, Ramamurthy V. Dwivedula, *Member, IEEE*, and Nilesh B. Siraskar

***Abstract*—A decentralized model reference adaptive controller (MRAC) for a class of large-scale systems with unmatched interconnections is developed in this paper. A novel reference model is proposed for the class of large-scale systems considered and a decentralized, full-state feedback adaptive controller is developed for each subsystem of the large-scale system. It is shown that with the proposed decentralized adaptive controller, the states of the subsystems can asymptotically track the desired reference trajectories. To substantiate the performance of the proposed controller, a large web processing line, which mimics most of the features of an industrial web process line, is considered for experimental study. Extensive experiments were conducted with the proposed decentralized adaptive controller and an often used decentralized industrial proportional–integral (PI) controller. A representative sample of the comparative experimental results is shown and discussed.**

***Index Terms*—Decentralized control, large-scale systems, material processing, model reference adaptive control (MRAC), tension control, web handling systems.**

I. Introduction

LARGE-SCALE interconnected systems appear in a variety of engineering applications such as power systems, large structures, manufacturing processes, communication systems, transportation systems, and large-scale economic systems. Decentralized control schemes present a practical and efficient means for designing control algorithms that utilize only the state of each subsystem without any information from other subsystems. The ease and flexibility of designing controllers for subsystems formed an important motivation for the design of decentralized schemes since information exchange between subsystems is not needed. Consequently, the decentralized adaptive control problem for large-scale systems received and continues to receive considerable attention in the literature in the last two decades (see, for example, [1]–[9]).

In [1], a survey of early results in decentralized control of large-scale systems was given. Stabilization and tracking using decentralized adaptive controllers was considered in [2] and sufficient conditions were established that guarantee boundedness and exponential convergence of errors; this result was provided for the case where the relative degree of the transfer function of each decoupled subsystem is less than or equal to 2. Decentralized control schemes that can achieve desired robust performance in the presence of uncertain interconnections can be found in [4]. A large body of literature in decentralized control of large-scale systems can be found in [5]. Considering systems with matched interconnections, in [6], it is shown that in strictly decentralized adaptive control systems, it is theoretically possible to asymptotically track the desired outputs with zero error. Decentralized output feedback control of large-scale systems can be found in [8] and references therein. Recent work on the use of neural networks in the control of large-scale interconnected systems may be found in [9].

In this research, we consider a new reference model for each subsystem that depends on the reference trajectory of the overall large-scale system; that is, there is coupling between individual subsystem reference models. As a result, the proposed design relies on the fact that each subsystem knows the reference trajectory of other subsystems in the design of its decentralized controller. Further, much of the past research has concentrated on the interconnections being matched. In this research, we consider a class of large-scale systems with unmatched interconnections; the web processing application, where the interconnections are unmatched, directly falls into this class.

To validate the control scheme proposed, a large-scale system is considered and the control scheme is implemented on it. The system considered for this purpose is a High Speed Web Line (HSWL) at Web Handling Research Center (WHRC), Oklahoma State University (OSU). HSWL is a state-of-the-art experimental platform that mimics most of the features of a real-life web process line and is, perhaps, a unique setup among most of the universities.

The contributions of the paper are the following. 1) A new model reference adaptive controller (MRAC) solution to a class of large-scale systems with unmatched interconnections is proposed. 2) The proposed MRAC solution is implemented on a state-of-the-art web handling experimental setup that mimics most of the features of a real-life web process line.

The remainder of the paper is organized as follows. Section II presents the problem statement and the new reference model. The problem of designing an asymptotically stable MRAC is reduced to that of finding a solution to the algebraic Riccati equation (ARE) in Section III and a local, full-state feedback controller for each subsystem is proposed. To validate the proposed controller, a state-of-the-art web handling experimental setup is considered for implementation. The experimental web platform is described in Section IV and the dynamic model of the experimental platform is presented in Section IV-A.

Manuscript received December 19, 2005; revised August 5, 2006. Recommended by Technical Editor C. Mavroidis. This work was supported in part by the National Science Foundation under Grant CMS 9982071 and in part by the Institute of Electrical and Electronics Engineers (IEEE).

P. R. Pagilla is with the School of Mechanical and Aerospace Engineering, Oklahoma State University, Stillwater, OK 74078-5016 USA (e-mail: pagilla@ceat.okstate.edu).

R. V. Dwivedula is with Fife Corporation, Oklahoma City, OK 73126 USA (e-mail: ram_dula@yahoo.com).

N. B. Siraskar is with Dexterous Technologies, Nashik, India (e-mail: nileshcentury@yahoo.com).

Digital Object Identifier 10.1109/TMECH.2007.892823

Comparative experimental results with the proposed MRAC design and the industrial proportional-integral (PI) controller are presented in Section V-A. Conclusions of the research are given in Section VI.

II. Problem Statement

We consider a large-scale system $\mathbb{S}$ consisting of $(N+1)$ subsystems; each subsystem $\mathbb{S}_i$ is described by

$$\mathbb{S}_i : \dot{x}_i(t) = A_i x_i(t) + B_i U_i(t) + \sum_{j=0, j\neq i}^{N} A_{ij} x_j(t), \qquad i = 0, 1, \ldots, N \qquad (1)$$

where $x_i(t) \in \mathbb{R}^{n_i}$ is the state of the ith subsystem and $U_i(t) \in \mathbb{R}$ is the input. Notice that the interconnection term (last term) in (1) is unmatched. The following assumptions are made in developing decentralized MRAC.

Assumption 1: (A_i, B_i) are controllable. That is, there exist vectors $k_i \in \mathbb{R}^{n_i}$ such that, for an asymptotically stable matrix A_{mi},

$$(A_i - A_{mi}) = B_i k_i^\top. \qquad (2)$$

Assumption 2: Subsystem matrices B_i are known and A_i are unknown.

Assumption 3: The interconnection matrices A_{ij} are known.

Assumptions 1 and 2 are standard in literature [6]. Assumption 3 is relevant to a class of systems. The significance and applicability of the assumptions become apparent in Section IV where a specific case of large-scale systems, viz., web processing lines is presented.

The entire large-scale system $\mathbb{S}$ can be represented by

$$\mathbb{S} : \dot{x}(t) = Ax(t) + BU(t) \qquad (3)$$

where $x^\top(t) = [x_0^\top(t),\ x_1^\top(t), \ldots, x_N^\top(t)]$, $U^\top(t) = [U_0(t), U_1(t), \ldots, U_N(t)]$, A is a matrix composed of block diagonal matrix elements A_i and off-diagonal matrix elements A_{ij}, and B is a block diagonal matrix composed of B_i. We assume that the pair (A, B) is controllable.

Existing research (see, for example, [2], [3], and [6]) has considered the decentralized MRAC problem for large-scale systems with a reference model given by

$$\dot{x}_{mi}(t) = A_{mi} x_{mi}(t) + B_i r_i(t) \qquad (4)$$

where $x_{mi}(t)$ are the reference state vectors and $r_i(t)$ are bounded reference inputs. In this research, we consider a different structure for the reference model by making use of the known interconnection matrices A_{ij} in the reference model. The reference model for each individual subsystem $\mathbb{S}_{mi}$ is described by the equations

$$\mathbb{S}_{mi} : \dot{x}_{mi}(t) = A_{mi} x_{mi}(t) + B_i r_i(t) - B_i k_{mi}^\top x_m + \sum_{j=0, j\neq i}^{N} A_{ij} x_{mj}(t) \qquad (5)$$

where $k_{mi} \in \mathbb{R}^n, n = n_0 + n_1 + \cdots + n_N$, and $x_m^\top(t) = [x_{m0}^\top, x_{m1}^\top, \ldots, x_{mN}^\top]$. With the structure for the reference model (5), the condition for existence of solution to the control problem can be specified in terms of the state matrices of the reference model A_{mi}, as given by (13) later.

The reason for including the term $B_i k_{mi}^\top x_m$ in (5) becomes clear when we consider the reference model for the entire large-scale system that is given by

$$\mathbb{S}_m : \dot{x}_m(t) = A_m x_m(t) + Br(t) - BK_m^\top x_m \qquad (6)$$

where $r^\top(t) = [r_0(t), r_1(t), \ldots, r_N(t)]$, $K_m = [k_{m0}, k_{m1}, \ldots, k_{mN}]$, and

$$A_m = \begin{bmatrix} A_{m0} & A_{01} & A_{02} & \cdots & A_{0N} \\ A_{10} & A_{m1} & A_{12} & \cdots & A_{1N} \\ \vdots & \vdots & \vdots & \vdots & \vdots \\ A_{N0} & A_{N1} & \cdots & \cdots & A_{mN} \end{bmatrix}.$$

Notice that if A_m is not stable for given A_{mi}, then one can place the eigenvalues of $A_m - BK_m^\top$ by choosing K_m to make the system in (6) stable. If A_m is asymptotically stable for given A_{mi}, then one can simply choose K_m to be the null matrix.

The goal is to design bounded decentralized control inputs $U_i(t)$ such that $x_i(t)$ are bounded and the error $e_i(t) = x_i(t) - x_{mi}(t)$ converges to zero, that is, $\lim_{t\to\infty} e_i(t) = 0$ for all $i \in I = \{0, 1, \ldots, N\}$. The controller proposed and proof of stability of the controller are presented in Section III.

III. Controller Design and Stability

A few definitions and results useful in the proof are given in Section III-A followed by the main result in Section III-B.

A. Preliminaries

Definition 1 ([10]): Suppose $A \in \mathbb{C}^{n\times n}$ has no eigenvalue on the imaginary axis. Let $U \subset \mathbb{C}^{n\times n}$ be the set of matrices with at least one eigenvalue on the imaginary axis. The distance from A to U is defined by

$$\delta_s(A) = \min\{\|E\| : A + E \in U\}. \qquad (7)$$

$\delta_s(A)$ has the property [10] that

$$\delta_s(A) = \overset{\min}{\omega \in \mathbb{R}} \sigma_{\min}(A - j\omega I). \qquad (8)$$

Lemma 1 ([10]): Let $\rho \geq 0$ and define

$$H_\rho = \begin{bmatrix} A & -\rho I \\ rhoI & -A^\top \end{bmatrix}. \qquad (9)$$

Then, H_ρ has an eigenvalue whose real part is zero if an only if $\rho \geq \delta_s(A)$. This theorem characterizes $\delta_s(\cdot)$ by

$$\delta_s(A) = \inf\{\rho : H_\rho \text{ is not hyperbolic}\}. \qquad (10)$$

Algorithms to compute $\delta_s(\cdot)$ are illustrated in [10]–[12].

Lemma 2 ([13], [14]): Consider the ARE

$$A^\top P + PA + PRP + Q = 0. \tag{11}$$

If $R = R^\top \geq 0, Q = Q^\top > 0$, A is Hurwitz, and the associated Hamiltonian matrix

$$\mathcal{H} = \begin{bmatrix} A & R \\ -Q & -A^\top \end{bmatrix}$$

is hyperbolic, i.e., $\mathcal{H}$ has no eigenvalues on the imaginary axis, then there exists a unique $P = P^\top > 0$, which is the solution of the ARE (11).

B. Main Result

Theorem 1: Given the large-scale system (1) and the reference model (5), there exists a positive definite matrix $P_i = P_i^\top$ such that the decentralized control law and the parameter updation law given by

$$U_i(t) = r_i(t) - k_{mi}^\top x_m(t) - \hat{k}_i^\top x_i(t) \tag{12a}$$

$$\dot{\hat{k}}_i(t) = -(e_i^\top(t) P_i B_i) x_i(t) \tag{12b}$$

where $\hat{k}_i$ is an estimate of k_i and e_i is the subsystem error given by $e_i \triangleq x_i - x_{mi}$, which render the closed-loop system asymptotically stable if

$$\delta_s(A_{mi}) > \sqrt{N\xi_i}. \tag{13}$$

Proof: Given the large-scale system (1) and the reference model (5), define subsystem error as $e_i(t) \triangleq x_i(t) - x_{mi}(t)$. Then, the error dynamics of the closed-loop system defined by (1), (5), (12) can be obtained as

$$\dot{e}_i(t) = A_{mi} e_i(t) + B_i \tilde{k}_i^\top(t) x_i(t) + \sum_{j=0, j\neq i}^{N} A_{ij} e_j(t) \tag{14}$$

where $\tilde{k} \triangleq k_i - \hat{k}$. Consider the following Lyapunov function candidate:

$$V(e_i, \tilde{k}_i) = \sum_{i=0}^{N} (e_i^\top P_i e_i + \tilde{k}_i^\top \tilde{k}_i). \tag{15}$$

The derivative of the Lyapunov function candidate along the trajectories of (14) and (12b) is given by

$$\dot{V}(e_i, \tilde{k}_i) = \sum_{i=0}^{N} \left\{ e_i^\top (A_{mi}^\top P_i + P_i A_{mi}) e_i + \sum_{j=0, j\neq i}^{N} [\underbrace{e_i^\top P_i}_{\alpha^\top} \underbrace{A_{ij} e_j}_{\beta} + \underbrace{e_j^\top A_{ij}^\top}_{\beta^\top} \underbrace{P_i e_i}_{\alpha}] \right\}. \tag{16}$$

Using the inequality $\alpha^\top \beta + \beta^\top \alpha \leq \alpha^\top \alpha + \beta^\top \beta$, $\forall \alpha, \beta \in \mathbb{R}^{n_i}$, for terms in braces in (16) and rearranging the terms, we obtain

$$\begin{aligned} \dot{V}(e_i, \tilde{k}_i) &\leq \sum_{i=0}^{N} \left\{ e_i^\top (A_{mi}^\top P_i + P_i A_{mi}) e_i + N e_i^\top P_i^2 e_i + e_i^\top \underbrace{\left(\sum_{j=0, j\neq i}^{N} A_{ij}^\top A_{ij} \right)}_{X_i} e_i \right\} \\ &\leq \sum_{i=0}^{N} \left\{ e_i^\top (A_{mi}^\top P_i + P_i A_{mi} + N P_i^2 + \xi_i I) e_i \right\} \end{aligned} \tag{17}$$

where $\xi_i \triangleq \lambda_{\max}(X_i)$. Therefore, if there exist symmetric positive definite matrices P_i such that

$$A_{mi}^\top P_i + P_i A_{mi} + P_i (NI) P_i + (\xi_i + \epsilon_i) I = 0 \tag{18}$$

for $\epsilon_i > 0$ then

$$\dot{V}(e_i, \tilde{k}_i) \leq -\sum_{i=0}^{N} \epsilon_i e_i^\top e_i \tag{19}$$

and $V(e_i, \tilde{k}_i)$ qualifies as a Lyapunov function and the equilibrium point $e_i = 0$ is asymptotically stable for all $i \in I$. Proof of Theorem 1 now rests on the existence of symmetric positive definite solution P_i to the ARE (18). To this end, we invoke Lemma 2. Define the Hamiltonian for the ARE (18) as

$$\mathcal{H}_i = \begin{bmatrix} A_{mi} & NI \\ -(\xi_i + \epsilon_i) I & -A_{mi}^\top \end{bmatrix}. \tag{20}$$

The eigenvalues of the Hamiltonian may be found by writing

$$\begin{aligned} \det(sI - \mathcal{H}_i) &= \begin{bmatrix} sI - A_{mi} & -NI \\ (\xi_i + \epsilon_i) I & sI + A_{mi}^\top \end{bmatrix} \\ &= \det \underbrace{[(sI + A_{mi})^\top (sI - A_{mi}) + N(\xi_i + \epsilon_i) I]}_{G(s)} = 0. \end{aligned} \tag{21}$$

From (21), it may be seen that $\mathcal{H}_i$ is hyperbolic if $G(j\omega)$ is nonsingular. Notice that

$$\begin{aligned} -G(j\omega) &= -(j\omega I + A_{mi})^\top (j\omega I - A_{mi}) - N(\xi_i + \epsilon_i) I \\ &= \underbrace{(A_{mi} - j\omega I)^H (A_{mi} - j\omega I)} - N(\xi_i + \epsilon_i) I. \end{aligned} \tag{22}$$

From (8), we see that the term in braces in (22) is always greater than $\delta_s^2(A_{mi}) I$. Thus, if

$$\delta_s^2(A_{mi}) - N\xi_i > 0 \tag{23}$$

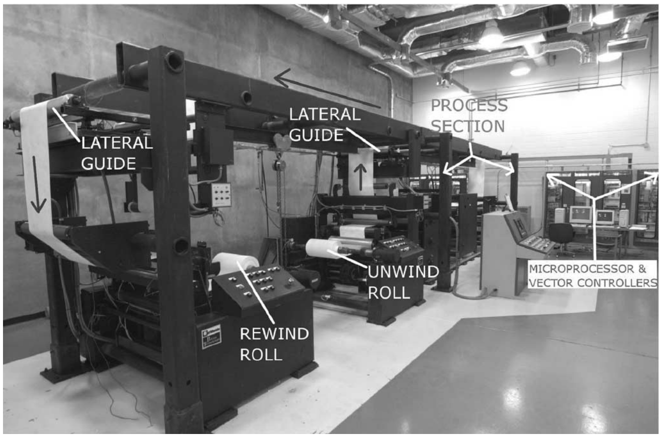

Fig. 1. Picture of the experimental web platform.

we can always choose a value for ϵ_i as $\gamma(\delta_s^2(A_{mi}) - N\xi_i)/N$ for some γ in the range $0 \leq \gamma \leq 1$ to make $-G(j\omega)$ in (22) positive definite (and, hence, make it hyperbolic), thus ensuring the existence of a symmetric positive definite P_i to satisfy the ARE (18).

The condition for existence of solution given in (23) is in terms of the matrix A_{mi} of the reference model (5) and the maximum eigenvalue of the matrix X_i defined in (17). Thus, given a large-scale system, a suitable reference model may be chosen to satisfy (23).

Section IV briefly presents details about the experimental platform considered for implementation of the proposed control algorithm, the dynamic model of the plant, and the experimental results.

IV. Web Processing Application

A web is any material that is manufactured and processed in continuous, flexible strip form. Examples include paper, plastics, textiles, strip metals, and composites. Web processing pervades almost every industry today. It allows us to mass produce a rich variety of products from a continuous strip material. Products that include web processing somewhere in their manufacturing include aircraft, appliances, automobiles, bags, books, diapers, boxes, newspapers, magnetic tapes, and many more. Typically, web process lines consist of an unwind section, one or more process sections, and a rewind section. Web tension and velocity in each of these sections are key variables that influence the quality of the finished web and, hence, the products manufactured from it.

Fig. 1 shows a picture of the experimental platform and Fig. 2 is a schematic showing the web-path and various sections in the experimental platform. It is possible, theoretically, to "decentralize" this large-scale system into subsystems in an arbitrary way. However, it is convenient if subsystems are chosen as physically identifiable segments in the system. Consequently, four "sections" are identified as subsystems in Fig. 2: 1) unwind section; 2) master speed section; 3) process section; and

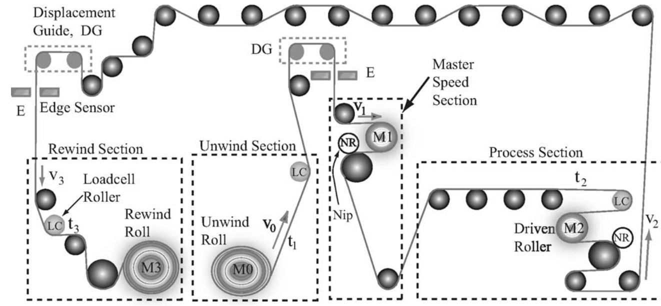

Fig. 2. Schematic of the experimental platform showing the web-path and various sections.

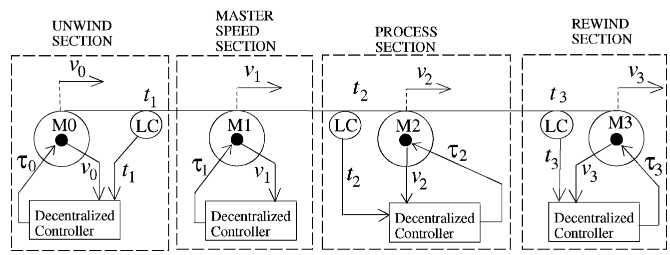

Fig. 3. Sketch of the platform showing driven rolls/rollers and tension zones.

4) rewind section. Each of these sections is equipped with a drive motor to impart velocity/tension to the web and sensors (loadcells for tension measurement and encoder or some other sensor for speed measurement). As the name indicates, the master speed section has a driven roller that is used to set the reference web transport speed for the entire web line, and is, generally, the first driven roller upstream of the unwind roll in almost all web process lines. The master speed section is not used to regulate the tension in the spans adjacent to it. Except the master speed section, all the other sections use two local feedback signals, namely, the web tension and web velocity; the master speed section uses only the web velocity as feedback signal.

Fig. 3 shows a line sketch of the decentralization scheme considered. In Fig. 3, M_0, M_2, and M_3 are the drive motors for the unwind section, process section, and the rewind section, and M_1 is the drive motor for master speed section. Except for M_1, the other motors use a tension feedback (from loadcell, indicated by LC in Fig. 3) and a speed feedback. Motors M_0 and M_3 in Fig. 3 are 30 brake horsepower (bhp), three-phase RPM ac motors under vector control whereas motors M_1 and M_2 are 15 bhp, three-phase RPM ac motors under analog HR-2000 control. The motor drive systems, the real-time architecture that includes micro-processors, I/O cards, and the real-time control environment AutoMax, and the other mechanical hardware are from Rockwell Automation. The lateral guides shown in Fig. 1 are Fife displacement guides. These guides are controlled independent of the real-time control software through dedicated controllers. The dynamics of each of the four sections is presented in the following sections.

A. Dynamic Model

The following table shows the notation used in this section.

E	Young's modulus of web material.
A	Area of cross section of web.
R_i	Radius of roller.
t_{ri}	ith section reference web tension.
v_{ri}	ith section reference web velocity.
J_i	Polar moment of inertia of roller.
n_i	Gear ratio (motor shaft to roller shaft).
L_i	Length of web span.
b_{fi}	Viscous friction coefficient.
T_i	ith section web tension error.
V_i	ith section web velocity error.

The dynamic models for each of the sections in Fig. 3, derived from the Newton's laws and conservation of mass principle in [15]–[18], are summarized in this section. Extensions of these models that include the inertia changes in the unwind/rewind and other devices such as dancers and accumulators can be found in [19]–[23].

Unwind section:

$$\frac{J_0}{R_0}\dot{v}_0 = t_1 R_0 - n_0 u_0 - \frac{b_{f0}}{R_0} v_0 - \frac{t_w}{2\pi R_0}\left(\frac{J_0}{R_0^2} - 2\pi\rho_w b_w R_0^2\right) v_0^2 \tag{24}$$

$$L_1 \dot{t}_1 = AE[v_1 - v_0] + t_0 v_0 - t_1 v_1 \tag{25}$$

where L_1 is the length of the web span between unwind roller (M_0) and master speed roller (M_1), A is the area of cross section of the web, E is the modulus of elasticity of the web material, and t_0 represents the wound-in tension of the web in the unwind roll.

Master speed roller:

$$\frac{J_1}{R_1}\dot{v}_1 = (t_2 - t_1)R_1 + n_1 u_1 - \frac{b_{f1}}{R_1} v_1. \tag{26}$$

Process section:

$$L_2 \dot{t}_2 = AE[v_2 - v_1] + t_1 v_1 - t_2 v_2 \tag{27}$$

$$\frac{J_2}{R_2}\dot{v}_2 = (t_3 - t_2)R_2 + n_2 u_2 - \frac{b_{f2}}{R_2} v_2. \tag{28}$$

Rewind section:

$$L_3 \dot{t}_3 = AE[v_3 - v_2] + t_2 v_2 - t_3 v_3 \tag{29}$$

$$\frac{J_3}{R_3}\dot{v}_3 = -t_3 R_3 + n_3 u_3 - \frac{b_{f3}}{R_3} v_3 + \frac{t_w}{2\pi R_3}\left(\frac{J_3}{R_3^2} - 2\pi\rho_w b_w R_3^2\right) v_3^2. \tag{30}$$

Equations (24) through (30) represent the dynamics of the web and rollers for the web line configuration shown in Fig. 3. Extension to other web lines can be easily made based on this model. For web process lines that have a series of process sections between the master speed roller and the rewind roll, then (27) and (28) can be written down for each process section.

V. Control Design

The control goal is to regulate web tension in each of the tension zones while maintaining the prescribed web transport velocity. The control input is computed in two steps:

Step I: The control input required to keep the web line at the forced equilibrium of the reference web tension (t_{ri}) and web velocity in each of the zones is computed. The equilibrium input compensates for the torque dissipated by viscous friction (e.g., $b_{f0}v_{r0}$) at reference web velocity and also for torque due to reference web tensions. It might be noted that, for the unwind roll, the radius changes as the web material is released. Thus, the torque due to reference web tension (e.g., $t_{r1}R_0$) changes. The computed equilibrium input to unwind roll accounts for the radius change leaving the other part of the control isolated from this change. A similar observation may be made for rewind roll.

Step II: Additional compensation to provide error convergence in the presence of disturbance is computed. The additional compensation is computed via a static state-feedback to achieve decentralized control scheme shown in Fig. 3.

Define the variables

$$T_i = t_i - t_{ri}$$
$$V_i = v_i - v_{ri}$$
$$\bar{U}_i = u_i - u_{i,\mathrm{eq}}, \qquad \text{for} \quad i = 0,1,2,3 \tag{31}$$

where t_{ri} and v_{ri} are tension and velocity references, respectively, and $u_{i,\mathrm{eq}}$ is the control input that maintains the forced equilibrium at the reference values. In the following, the equilibrium control inputs and reference velocities are determined for each driven roll/roller based on the reference velocity of the master speed roller and reference tension in each tension zone.

Using the definitions of the variables, the velocity dynamics of the unwind section, that is, (24), may be written as

$$\frac{J_0}{R_0}\dot{V}_0 = (T_1 + t_{r1})R_0 - n_0(\bar{U}_0 + u_{0\mathrm{eq}}) - \frac{b_{f0}}{R_0}(V_0 + v_{r0}) \underbrace{- \frac{t_w}{2\pi R_0}\left(\frac{J_0}{R_0^2} - 2\pi\rho_w b_w R_0^2\right)(V_0 + v_{r0})^2}_{f_0(V_0)} \tag{32}$$

where the derivative of the reference velocity $\dot{v}_{r0}$ is taken to be zero since the web velocity needs to be maintained constant. At forced equilibrium position, $t_1 = t_{r1}$, $v_0 = v_{r0}$, and $u_0 = u_{0,\mathrm{eq}}$. Hence, $T_1 = 0$, $V_0 = 0$, and $\bar{U}_0 = 0$. Substituting this into (32), the equilibrium input for the unwind roll is computed as

$$u_{0,\mathrm{eq}} = -\frac{b_{f0}}{n_0 R_0} v_{r0} + \frac{R_0}{n_0} t_{r1} - \frac{t_w}{2\pi n_0 R_0}\left(\frac{J_0}{R_0^2} - 2\pi\rho_w b_w R_0^2\right) v_{r0}^2. \tag{33}$$

Notice that the equilibrium input for the unwind roll depends on the unwind roll radius that can be updated in real time. Similarly, the equilibrium inputs for other sections may be computed as

$$u_{1,\text{eq}} = \frac{b_{f1}}{n_1 R_1} v_{r1} - \frac{R_1}{n_1}(t_{r2} - t_{r1}) \tag{34}$$

$$u_{2,\text{eq}} = \frac{b_{f2}}{n_2 R_2} v_{r2} - \frac{R_2}{n_2}(t_{r3} - t_{r2})$$

$$u_{3,\text{eq}} = \frac{b_{f3}}{n_3 R_3} v_{r3} + \frac{R_3}{n_3} t_{r3} \tag{35}$$

$$+ \frac{t_w}{2\pi n_3 R_3}\left(\frac{J_3}{R_3^2} - 2\pi \rho_w b_w R_3^2\right) v_{r3}^2. \tag{36}$$

If the equilibrium inputs given by (33)–(36) are applied by the drive motors, the tension in each of the sections will be t_{ri}, the reference tension. The reference velocities to be specified for each of the sections may be computed by using the known reference tensions and the tension dynamics. For example, the dynamics of the unwind section may be written as

$$L_1 \dot{T}_1 = AE[(V_1 + v_{r1}) - (V_0 + v_{r0})] + t_0(V_0 + v_{r0}) - (T_1 + t_{r1})(V_1 + v_{r1}). \tag{37}$$

At equilibrium, $\dot{T}_1 = T_1 = V_0 = V_1 = 0$ and, hence,

$$v_{r0} = \frac{AE - t_{r1}}{AE - t_0} v_{r1}. \tag{38}$$

In simplifying (37), it is assumed that the product terms $(T_i V_i)$ are much smaller than the terms with EA as coefficient and, hence, are negligible. This assumption is practical both for metal webs as well as nonmetal webs.

Similarly, the reference velocities for other sections may be specified in terms of the velocity reference for master speed section as

$$v_{r2} = \left(\frac{AE - t_{r1}}{AE - t_{r2}}\right) v_{r1} \tag{39}$$

$$v_{r3} = \left(\frac{AE - t_{r1}}{AE - t_{r3}}\right) v_{r1}. \tag{40}$$

Thus, if the reference tensions are specified as t_{ri}, reference velocities are specified as v_{ri} satisfying (38)–(40), and the equilibrium inputs given by (33)–(36) are applied, then the process line is maintained in forced equilibrium state in the absence of any perturbations. Additional compensation to ensure error convergence in the presence of perturbations is designed as follows.

Define

$$f_i(V_i) = \begin{cases} \frac{t_w}{2\pi n_i R_i}\left(\frac{J_i}{R_i^2} - 2\pi\rho_w b_w R_i^2\right)(V_i^2 + 2V_i v_{ri}), & \text{for } i = 0,3 \\ 0, & \text{for } i = 1,2 \end{cases} \tag{41}$$

and

$$\bar{U}_i = U_i - f_i(V_i) \tag{42}$$

where the term $f_i(V_i)$ appearing in (32) and (42) compensates for the change in the inertia of the unwind/rewind rolls. Further, define the state vector for the unwind section as $x_0^T = [T_1, V_0]$ and the state for the master speed roller as $x_1 = V_1$. After master speed section, define the state vector for the jth subsystem as $x_j^T = [T_j, V_j]$ for $j = 2, 3$. With the definitions given in (41) and (42), and the state variables defined, the dynamics of the four sections of the process line may be written as follows.

Unwind section:

$$\dot{x}_0 = \begin{bmatrix} \dot{T}_1 \\ \dot{V}_0 \end{bmatrix} = A_0 x_0 + B_0 U_0 + \sum_{j=1}^{3} A_{0j} x_j \tag{43}$$

where A_{02} and A_{03} are null matrices, and

$$A_0 = \begin{bmatrix} -v_{r1}/L_1 & (t_0 - AE)/L_1 \\ R_0^2/J_0 & -b_{f0}/J_0 \end{bmatrix}$$

$$B_0 = \begin{bmatrix} 0 \\ -n_0 R_0/J_0 \end{bmatrix}$$

$$A_{01} = [(AE - t_{r1})/L_1, 0]^\top.$$

Master speed section:

$$\dot{x}_1 = \dot{V}_1 = A_1 x_1 + B_1 U_1 + \sum_{j=0, j\neq 1}^{3} A_{1j} x_j \tag{44}$$

where $A_1 = -b_{f1}/J_1,\ B_1 = n_1 R_1/J_1$, and

$$A_{10} = \left[\frac{-R_1^2}{J_1}, 0\right] \quad A_{12} = \left[\frac{R_1^2}{J_1}, 0\right] \quad A_{13} = [0, 0].$$

Process section:

$$\dot{x}_2 = \begin{bmatrix} \dot{T}_2 \\ \dot{V}_2 \end{bmatrix} = A_2 x_2 + B_2 U_2 + \sum_{j=0, j\neq 2}^{3} A_{2j} x_j \tag{45}$$

where

$$A_2 = \begin{bmatrix} -v_{r2}/L_2 & (AE - t_{r2})/L_2 \\ -R_2^2/J_2 & -b_{f2}/J_2 \end{bmatrix} \quad B_2 = \begin{bmatrix} 0 \\ n_2 R_2/J_2 \end{bmatrix}$$

$$A_{20} = \begin{bmatrix} v_{r1}/L_2 & 0 \\ 0 & 0 \end{bmatrix} A_{21} = \begin{bmatrix} (t_{r1} - AE)/L_2 \\ 0 \end{bmatrix}$$

$$A_{23} = \begin{bmatrix} 0 & 0 \\ R_2^2/J_2 & 0 \end{bmatrix}.$$

Rewind section:

$$\dot{x}_3 = \begin{bmatrix} \dot{T}_3 \\ \dot{V}_3 \end{bmatrix} = A_3 x_3 + B_3 U_3 + \sum_{j=0, j\neq 3}^{3} A_{3j} x_j \tag{46}$$

where A_{30} and A_{31} are null matrices, and

$$A_3 = \begin{bmatrix} -v_{r3}/L_3 & (AE - t_{r3})/L_3 \\ -R_3^2/J_3 & -b_{f3}/J_3 \end{bmatrix} \quad B_3 = \begin{bmatrix} 0 \\ n_3 R_3/J_3 \end{bmatrix}$$

$$A_{32} = \begin{bmatrix} v_{r2}/L_3 & (t_{r2} - AE)/L_3 \\ 0 & 0 \end{bmatrix}.$$

Equations (43)–(46) defining the dynamics of the four sections have the same form as the dynamics of the subsystems considered in (1). Hence, the control law given in (12) may be used to find U_i and the control input to the motor may be computed as

$$u_i = u_{i,\text{eq}} + U_i - f_i(V_i). \tag{47}$$

Notice that the elements of the interconnection matrices A_{ij} and the elements of the input matrices B_i involve the radii of rollers,

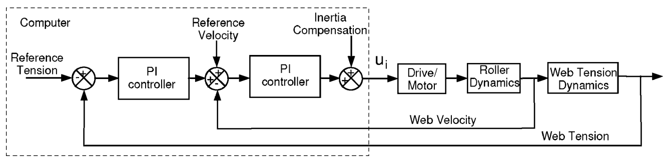

Fig. 4. Decentralized control strategy with two PI controllers.

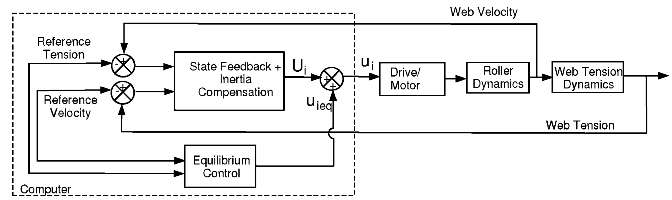

Fig. 5. Decentralized control strategy with proposed controller.

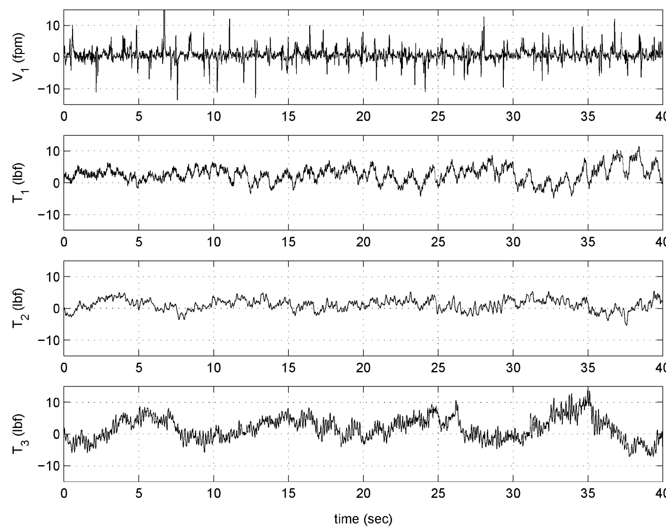

Fig. 6. Decentralized PI controller: reference velocity 1000 ft/min.

the polar moments of inertia, the reference tension/velocity, gearing ratio between the drive motor and the driven roller, and the web material properties. These quantities are known in advance and, thus, Assumption 3 applies to this plant. However, the system matrices A_i contain a term with coefficient of viscous friction that is unknown. It may further be noted that the interconnection terms in (43)–(46) are unmatched. This aspect is in direct contrast with that in [6] and [7], wherein the interconnections are matched. The control scheme presented in this paper takes advantage of the known interconnections to propose a decentralized control scheme to compensate for unmatched interconnections.

A. Experiments

To evaluate the effectiveness of the proposed controller, two sets of experiments were conducted. In the first set of the experiments, a control scheme using PI controllers, which are currently used in most of the web process lines, are used. This control scheme incorporates a tension control loop and a velocity control loop for each section (except for the master speed section that uses only a speed control loop). Though this scheme is very simple to implement, its performance is often limited and tuning the P and I gains is a tedious process. In the second set of experiments, the proposed controller is used. Experimental results with these control schemes show that the proposed control scheme offers a marked improvement in terms of lesser web tension error. A brief description of the decentralized PI control scheme is given in Section V-A.1. The results of experiments with PI control scheme are presented in Section V-A.2 and the results of experiments with the proposed controller are presented in Section V-A.3.

1) Decentralized PI-Control Scheme: In most industrial web process lines, the decentralized control scheme for each section has two cascaded PI control loops, as shown in Fig. 4. Notice that the PI action is not acting on tension and velocity errors individually; the output of the tension loop becomes a vernier correction term for the velocity loop.

It may be noted that this scheme utilizes two sensor signals: the web speed inferred from the tachometer mounted on the motor and the web tension inferred from the loadcell mounted on the roller. Though this scheme is used extensively in industrial web process lines, tuning the gains of the PI-controllers is a tedious process.

The implementation strategy for the proposed decentralized controller is shown in Fig. 5. Notice that the proposed scheme and the decentralized PI-control scheme utilize the same sensing information, namely, the web-tension signal from the loadcell and the web-speed signal from the encoders.

2) Results With PI Control Scheme: A series of experiments were conducted using the PI control scheme at different reference web tensions and different reference web velocities. In each case, the PI controllers were tuned carefully to yield best possible performance. As a representative sample, results of experiments conducted with PI control scheme at 1000 and 1500 ft/min are presented. The reference web tension in each case was set to 14.35 lbf. Fig. 6 shows the web velocity error at master speed section and the web tension error at each section for a reference web velocity of 1000 ft/min. The top plot in Fig. 6 shows the velocity error at master speed section. The subsequent plots in the figure show the tension error at each section. It can be seen from Fig. 6 that there is a considerable deviation of web tension from reference tension. Such variations in web tension are undesirable since they deteriorate the quality of the product made from web. Similar observation can be made from Fig. 7 that shows the results of experiments with a reference web velocity of 1500 ft/min.

3) Results With Proposed Controller: In the second set of experiments, the proposed controller is used to regulate the web velocity and tension in each zone with the same reference web velocities and reference web tensions under same conditions. Numerical values of various parameters used in the control design are presented in Table 1.

The matrices A_{mi} are chosen as follows.

Unwind section:

$$A_{m0} = \begin{bmatrix} -v_{r0}/L_1 & (AE - t_0)/L_1 \\ C_{01} & -C_{02} \end{bmatrix}$$

where $C_{01} = 120$ and $C_{02} = 2000$.

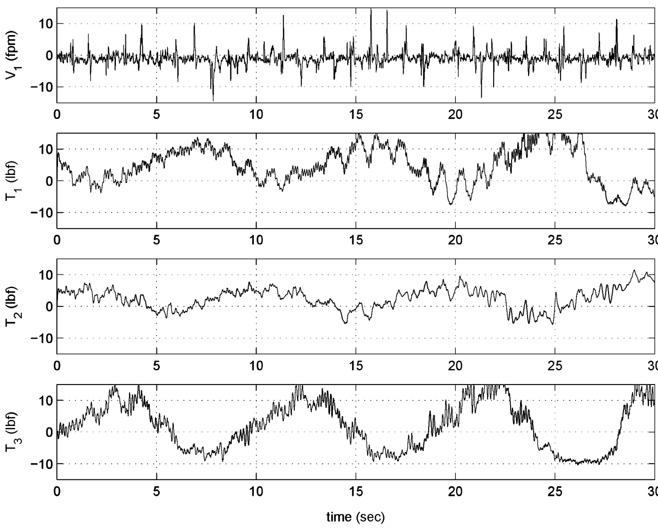

Fig. 7. Decentralized PI controller: reference velocity 1500 ft/min.

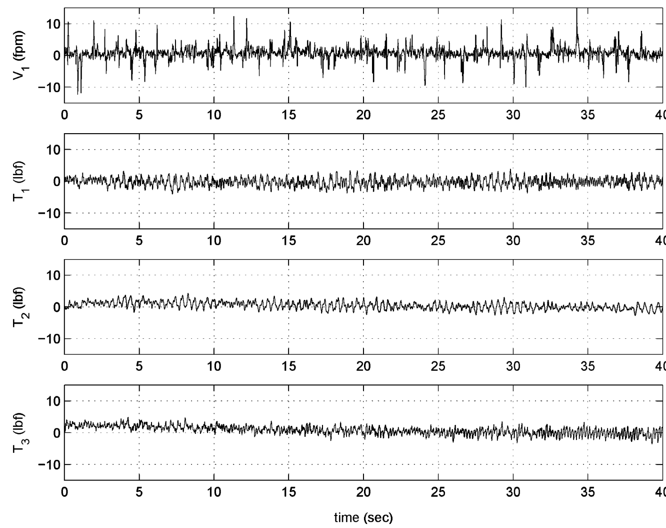

Fig. 8. Decentralized adaptive controller: reference velocity 1000 ft/min.

TABLE I
NUMERICAL VALUE OF PARAMETERS

v_{ri} (fpm) 1000	t_{ri} (lbf) 14.35	L_1 (ft) 20	L_2 (ft) 33	L_3 (ft) 67	J_0 (lb-ft^2) 8
J_1 (lb-ft^2) 2	J_2 (lb-ft^2) 2	J_3 (lb-ft^2) 4	AE (lbf) 2000	n_0, n_3 – 0.5	n_1, n_2 – 1
R_0 (ft) 1.25	R_1 (ft) 0.339	R_2 (ft) 0.339	R_3 (ft) 0.67		

Master speed section:

$$A_{m1} = C_{12} = 4000.$$

Process and rewind sections:

$$A_{mi} = \begin{bmatrix} -v_{ri}/L_i & (AE - t_{ri})/L_i \\ -C_{i1} & -C_{i2} \end{bmatrix}, \qquad i = 2, 3$$

where $C_{21} = 1500, C_{22} = 400, C_{31} = 15$, and $C_{32} = 15$.

It is verified that the condition given in (23) is satisfied for the given matrices A_{mi}. The linear quadratic regulator (LQR) algorithm is used to obtain the feedback gain k_m, which ensures that the reference states go to their desired values in an optimal sense. The optimal feedback gain k_m for a speed of 1000 ft/min is obtained as

$$k_m = \begin{bmatrix} k_{m0} \\ k_{m1} \\ k_{m2} \\ k_{m3} \end{bmatrix} = \begin{bmatrix} -433.2 & 70.0 & 3.6 & 12.3 \\ 792.2 & -63.0 & -1.8 & -12.5 \\ -232.5 & 37.3 & 1.2 & -3.7 \\ -19.8 & -4.3 & -20.4 & 630.5 \\ -0.3 & 0.1 & 187.9 & -1.2 \\ -36.8 & -3.2 & -100.8 & 1236.9 \\ -3.1 & -0.3 & -1.6 & 2984.9 \end{bmatrix}^{\top}. \tag{48}$$

The aforementioned values of C_{ij} and K_m are computed for reference web velocities of 1000 and 1500 ft/min, and a reference web tension of 14.35 lbf and controller given in (12) is implemented.

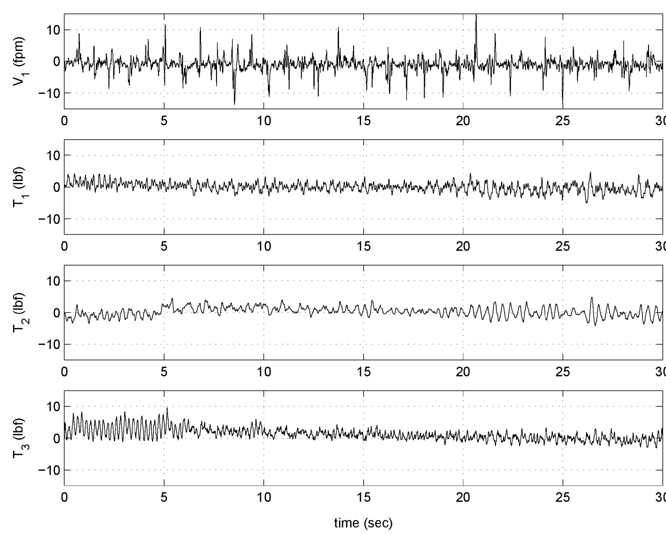

Fig. 9. Decentralized adaptive controller: reference velocity 1500 ft/min.

Fig. 8 shows experimental results conducted at a reference web velocity of 1000 ft/min. The top plot in Fig. 8 shows the web velocity error at master speed section and the subsequent plots show web tension errors at each section. It can be seen that there is a dramatic reduction in the amplitude of tension errors—to the tune of 75%—at each section. Similarly, Fig. 9 shows the results of the experiment for a reference web velocity of 1500 ft/min. It can be seen that a remarkable reduction in the web tension error is achieved in this case also.

Further, Figs. 10–13 show the adapted gains when the web speed is 1500 ft/min. All the estimated gains are initialized to zero at the beginning and, as the adaptation progresses, the gain estimates reach a final value to realize asymptotic stability of the overall system. Notice that the gains reach a final value and stay within a tolerance band very quickly. Also, it may be seen that the web-tension gains shown in Fig. 11 are negative.

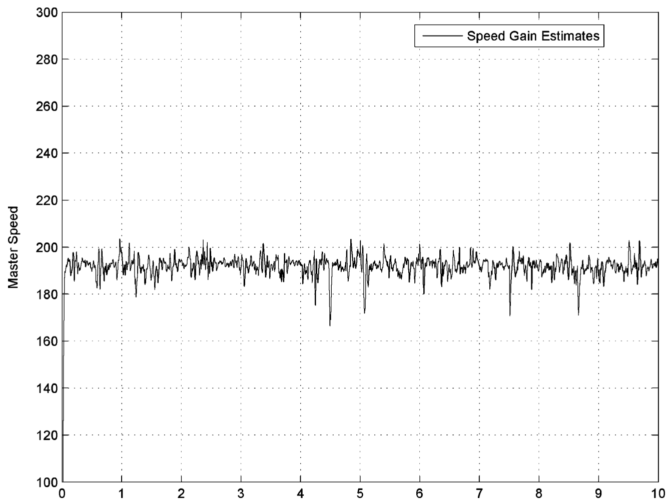

Fig. 10. Adaptive gains for master-speed section: 1500 ft/min.

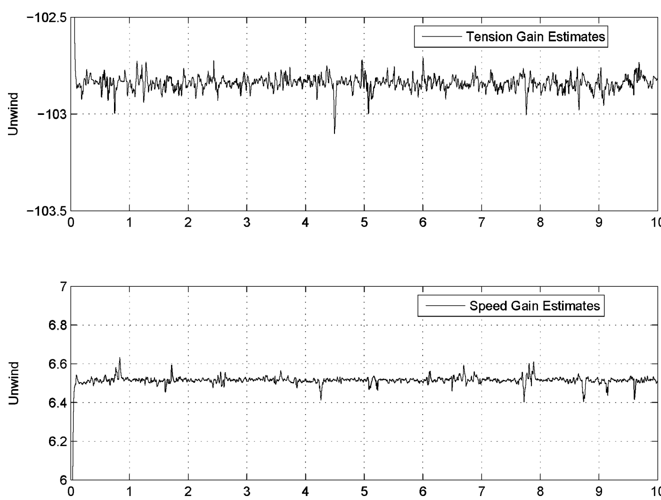

Fig. 11. Adaptive gains for unwind section: 1500 ft/min.

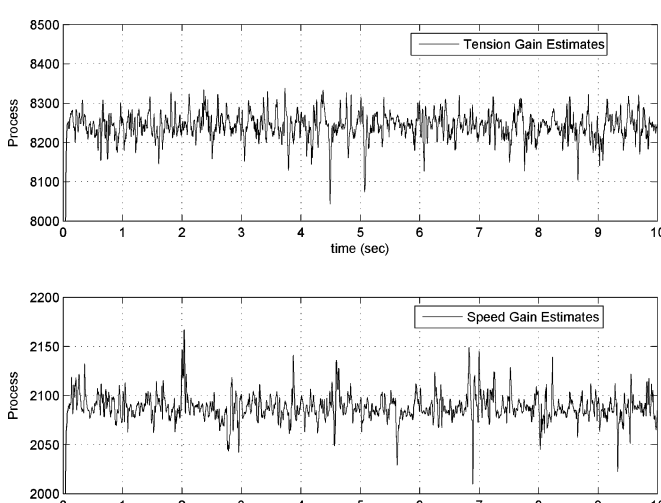

Fig. 12. Adaptive gains for process section: 1500 ft/min.

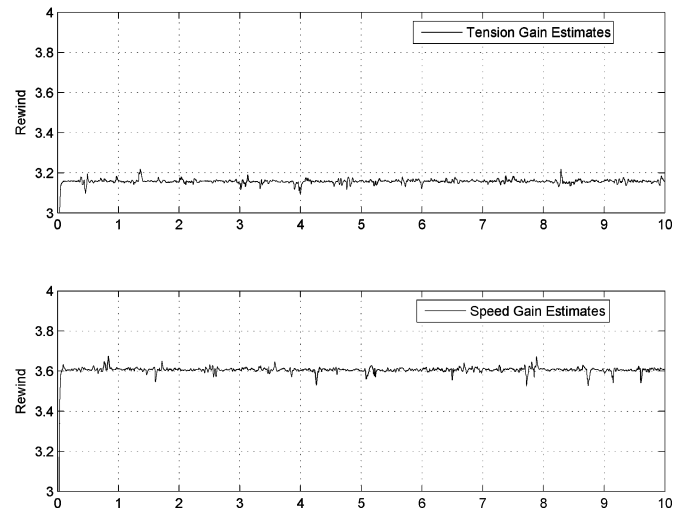

Fig. 13. Adaptive gains for winder section: 1500 ft/min.

This is because, the unwind motor is "braking" to keep the required tension and, thus, the torque exerted by unwind-motor is opposite to the torque exerted by other motors.

VI. Conclusion

Decentralized adaptive controller design for a class of large-scale systems with unmatched interconnections is investigated. A new reference model that includes known interconnections is considered and a stable decentralized MRAC design is proposed. Full-state feedback for each individual subsystem is used in the design of the decentralized control strategy. A large experimental web line is used for evaluating the proposed decentralized design. Comparative experimental results with an often used industrial PI controller show that the proposed decentralized design gives improved regulation of web tension. Several issues, such as unknown interconnections, extending the study to the case of output feedback, and conducting experiments with these cases, may be considered as important extensions of the work reported in this paper.

References

[1] N. R. Sandell, P. Varaiya, M. Athans, and M. G. Safonov, "Survey of decentralized control methods for large scale systems," *IEEE Trans. Autom. Control*, vol. AC-23, no. 2, pp. 108–128, Apr. 1978.

[2] P. A. Ioannou, "Decentralized adaptive control of interconnected systems," *IEEE Trans. Autom. Control*, vol. AC-31, no. 4, pp. 291–298, Apr. 1986.

[3] D. T. Gavel and D. D. Siljak, "Decentralized adaptive control: Structural conditions for stability," *IEEE Trans. Autom. Control*, vol. 34, no. 4, pp. 413–426, Apr. 1989.

[4] M. Ikeda, "Decentralized control of large scale systems," in *Three Decades of Mathematical System Theory*. New York: Springer-Verlag, 1989, pp. 219–242.

[5] D. D. Siljak, *Decentralized Control of Complex Systems*. New York: Academic, 1991.

[6] K. S. Narendra and N. O. Oleng, "Exact output tracking in decentralized adaptive control systems," *IEEE Trans. Autom. Control*, vol. 47, no. 2, pp. 390–395, Feb. 2002.

[7] B. M. Mirkin and P.-O. Gutman, "Decentralized output-feedback MRAC of linear state delay systems," *IEEE Trans. Autom. Control*, vol. 48, no. 9, pp. 1613–1619, Sep. 2003.

[8] Y. Zhang, C. Wen, and Y. Soh, "Robust decentralized adaptive stabilization of interconnected systems with guaranteed transient performance," *Automatica*, vol. 36, pp. 907–915, 2000.

[9] S. Huang, K. Tan, and T. Lee, "Nonlinear adaptive control of interconnected systems using neural networks," *IEEE Trans. Neural Netw.*, vol. 17, no. 1, pp. 243–246, Jan. 2006.

[10] R. Byers, "A bisection method for measuring the distance of a stable matrix to the unstable matrices," *SIAM J. Sci. Stat. Comput.*, vol. 9, pp. 875–881, 1988.

[11] C. He and G. A. Watson, "An algorithm for computing the distance to instability," *SIAM J. Matrix Anal. Appl.*, vol. 20, no. 1, pp. 101–116, 1998.

[12] C. V. Loan, "How near is a stable matrix to an unstable matrix," *Contemporary Math.*, vol. 45, pp. 456–477, 1985.

[13] M. A. Shayman, "Geometry of the algebraic Riccati equation, Part I," *SIAM J. Control Optim.*, vol. 21, pp. 375–394, May 1983.

[14] C. Aboky, G. Sallet, and J.-C. Vivalda, "Observers for Lipschitz nonlinear systems," *Int. J. Control*, vol. 75, no. 3, pp. 204–212, 2002.

[15] G. Brandenburg, "The dynamics of elastic webs threading a system of rollers," *Newspaper Tech.*, pp. 12–25, Sep. 1972.

[16] D. Whitworth, "Tension variations in pliable material in production machinery," Ph.D. dissertation, Loughborough Univ. Technol., Leicestershire, U.K., 1979.

[17] D. Whitworth and M. Harrison, "Tension variations in pliable material in production machinery," *J. Appl. Math. Model.*, vol. 7, pp. 189–196, Jun. 1983.

[18] J. J. Shelton, "Dynamics of web tension control with velocity or torque control," in *Proc. Amer. Control Conf.*, 1986, pp. 1–5.

[19] P. R. Pagilla, S. Garimella, L. Dreinhoefer, and E. King, "Dynamics and control of accumulators in continuous strip processing lines," in *Proc. IEEE Ind. Appl. Conf.*, vol. 4, May/Jun. 2000, pp. 2647–2653.

[20] P. R. Pagilla, "Modeling and advanced control of web handling systems," Oklahoma State Univ., Stillwater, Tech. Rep., Dec. 2000.

[21] P. R. Pagilla, S. S. Garimella, L. H. Dreinhoefer, and E. O. King, "Dynamics and control of accumulators in continuous strip processing lines," *IEEE Trans. Ind. Appl.*, vol. 37, no. 3, pp. 934–940, May/Jun. 2001.

[22] P. R. Pagilla, I. Singh, and R. V. Dwivedula, "A study on control of accumulators in web processing lines," *Trans. ASME, J. Dyn. Syst., Meas. Control*, vol. 126, pp. 453–461, Sep. 2004.

[23] P. R. Pagilla, N. B. Siraskar, and R. V. Dwivedula, "Decentralized control of web processing lines," *IEEE Trans. Control Syst. Technol.*, vol. 15, no. 1, pp. 106–117, Jan. 2007.

Prabhakar R. Pagilla (SM'91–M'96) received the B.Eng. degree from Osmania University, Hyderabad, India, in 1990, and the M.S. and Ph.D. degrees from the University of California, Berkeley, in 1994 and 1996, respectively, all in mechanical engineering.

He is currently a Professor in the School of Mechanical and Aerospace Engineering, Oklahoma State University, Stillwater. His current research interests include the areas of large-scale systems, adaptive control, mechatronics, disc drives, biomedical systems, and web handling systems. He is an Associate Editor of the *ASME Journal of Dynamic Systems, Measurement and Control* and a Technical Editor of the IEEE/ASME TRANSACTIONS ON MECHATRONICS.

Prof. Pagilla received a National Science Foundation CAREER Award in 2000.

Ramamurthy V. Dwivedula (S'05–M'06) received the B.Eng. degree from Andhra University, Visakhapatnam, India, in 1987, the M.Tech. degree from Indian Institute of Technology, New Delhi, India, in 1992, and the Ph.D. degree from Oklahoma State University, Stillwater, in 2006, all in mechanical engineering.

He is currently a Research and Development Mechanical Engineer at Fife Corporation, Oklahoma City, OK. His current research interests include adaptive control, web tension/speed control, and dancer systems to reject tension disturbances.

Nilesh B. Siraskar received the B.Eng. degree from the Government College of Engineering, Pune, India, in 2002, and the M.S. degree from Oklahoma State University, Stillwater, in 2004, both in mechanical engineering.

He was a Control Systems Engineer with Metro Automation, Dallas, TX. He is currently CEO of Dexterous Technologies, Nashik, India, where he is engaged in producing servo control systems for ac and dc motors. His current research interests include the areas of large-scale systems, adaptive control, mechatronics, and web handling systems.

Mr. Siraskar received the Graduate Research Excellence Award from Oklahoma State University in 2005.